The 2019 World Congress on
Advances in Structural Engineering and Mechanics (ASEM19)
Jeju Island, Korea, September 17 - 21, 2019

Tunnel Ahead Prediction on Tunnel Face and Side

Chang-Ho Hong[1)], Min-Hyeong Lee[2)], Gye-Chun Cho[3)]*, and Hee-Hwan Ryu[4)]

[1), 2), 3)] *Department of Civil and Environmental Engineering, KAIST, Daejeon 34141, Korea*
[4)] *Structural & Seismic Tech. Group, Next Generation Transmission & Substation Laboratory, KEPCO Research Institute*
[1)] hello-hch@kaist.ac.kr. [2)] apap0604@kaist.ac.kr, [3)] gyechun@kaist.ac.kr
[4)] hhryu82@kepco.co.kr

ABSTRACT

Site investigations have been performed to identify the abnormal ground prior to the tunnel construction for safety. However, site investigation cannot give an exact ground condition in deep and small diameter tunnels because the number of coring is restricted in deep depth. To overcome this problem, tunnel ahead prediction during the construction such as probe drilling, seismic and electromagnetic methods have been conducted. Among them, electromagnetic methods are most suitable for the tunnel ahead prediction since the probe drilling take time and cost and seismic methods generate the vibration that can raise the stability problem. The electrodes of the electromagnetic methods are commonly installed on the tunnel face. However, the number of the electrodes that can be installed on the tunnel face is limited in TBM tunneling because of the relatively small diameter of TBM tunnels in South Korea. The electrodes are installed both on the tunnel face and the side wall to extend the prediction depth and to reduce the number of the electrodes on the tunnel face. Theoretical equation is derived for the aforementioned electrode array. The laboratory tests were conducted to verify the derived equation.

1. INTRODUCTION

The site investigation such as coring and DC electrical resistivity survey on the surface is frequently conducted to predict the abnormal grounds along the tunnel line before construction. However, not all abnormal grounds are predicted from the site investigation because the number and method of the site investigation is determined based on the costs, the geology, and the topography (Rowe 1972). Tunnel ahead prediction methods such as probe drilling, seismic and electromagnetic methods have been utilized for safe tunnel construction. Among them, electromagnetic methods have advantages on conductive anomaly such as water-bearing sediment prediction (Li et al.

[1)] Post Doctoral Researcher
[2)] Graduate Student
[3)] Professor
[4)] Senior researcher

2017).

The electrodes for tunnel ahead prediction are usually installed on the tunnel face in tunneling with NATM method. However, the approach to the tunnel face is difficult in tunneling with TBM. Furthermore, more than 60% of the shield TBM whose diameter is smaller than 5 m is utilized in Seoul, South Korea (Jung et al., 2011). Therefore, the prediction range becomes decreased because prediction range of electromagnetic methods is closely related with the spacing of the electrodes (Roy and Apparrao 1971). The alternative electrode arrangement which installs the electrodes both on the tunnel face and side wall was suggested to overcome those two problems (Schaeffer and Mooney 2016). However, the complex data inversion procedure or numerical simulation should be conducted to interpret data since there is no theoretical equations for this electrode arrangement.

Therefore, this study tried to suggest the analytical solution of the electrical resistivity for the electrodes both on the tunnel face and side wall. The derived equation is verified with the experimental tests.

2. THEORETICAL STUDY

2.1 Electrical resistance of uniform medium

The electric potential at the distance *s* can be expressed by the following equation (Van Nostrand and Cook 1966):

$$V = \int_s^\infty \frac{\rho I}{2\pi x^2} dx = \frac{\rho I}{2\pi s} \tag{3}$$

where V is an electric potential at a distance s, ρ is the electrical resistivity of the medium, and I is an electric current through the medium.

Target geometry of the electrodes is that one is on the face of a TBM and the other is on the wall of a TBM (Fig 1(a)). The electrical resistance between two electrodes can be derived by the potential difference from each electrodes. The section of the tunnel is assumed as a hexagonal shape. The potentials from the face (V_1) and side electrode (V_2) is obtained by separating the integration range (Fig. 1(b)):

$$V_1 = \underbrace{\frac{\rho I}{2\pi}\left(\frac{1}{r} - \frac{1}{d/2}\right)}_{\mathrm{A_1(x)\ in\ Fig.\ 2(a)}} + \underbrace{\frac{\rho I}{4\pi(B-A)}\left(\ln\left(\frac{h+d/2-2r+A}{h+d/2-2r+B}\right) - \ln\left(\frac{d/2+A}{d/2+B}\right)\right)}_{\mathrm{A_1(x)+A_2(x)\ in\ Fig.\ 2(a)}} \tag{4}$$

$$V_2 = \left\{ \begin{array}{l} \underbrace{-\frac{\rho I}{\frac{8}{3}\pi}\left(\frac{1}{r} - \frac{1}{d/2}\right)}_{\mathrm{A_3(x)\ in\ Fig.\ 2(b)}} \underbrace{-\frac{\rho I}{\frac{10\pi}{3}(B-A)}\left[\ln\left(\frac{d+C}{d+D}\right) - \ln\left(\frac{d/2+C}{d/2+D}\right)\right]}_{\mathrm{A_4(x)\ in\ Fig.\ 2(b)}} \\ \underbrace{-\frac{\rho I}{4\pi(F-E)}\left[\ln\left(\frac{3d/2+E}{3d/2+F}\right) - \ln\left(\frac{d+E}{d+F}\right)\right]}_{\mathrm{A_5(x)\ in\ Fig.\ 2(b)}} \underbrace{-\frac{\rho I}{\frac{10}{3}\pi(H-G)}\left[\ln\left(\frac{h+G}{h+H}\right) - \ln\left(\frac{3d/2+G}{3d/2+H}\right)\right]}_{\mathrm{A_6(x)\ in\ Fig.\ 2(b)}} \\ \underbrace{-\frac{\rho I}{4\pi(K-J)}\left[\ln\left(\frac{h+d/2+J}{h+d/2+K}\right) - \ln\left(\frac{h+J}{h+K}\right)\right]}_{\mathrm{equipotential\ surface\ area\ containing\ both\ the\ tunnel\ wall\ and\ the\ tunnel\ face}} \end{array} \right\} \tag{5}$$

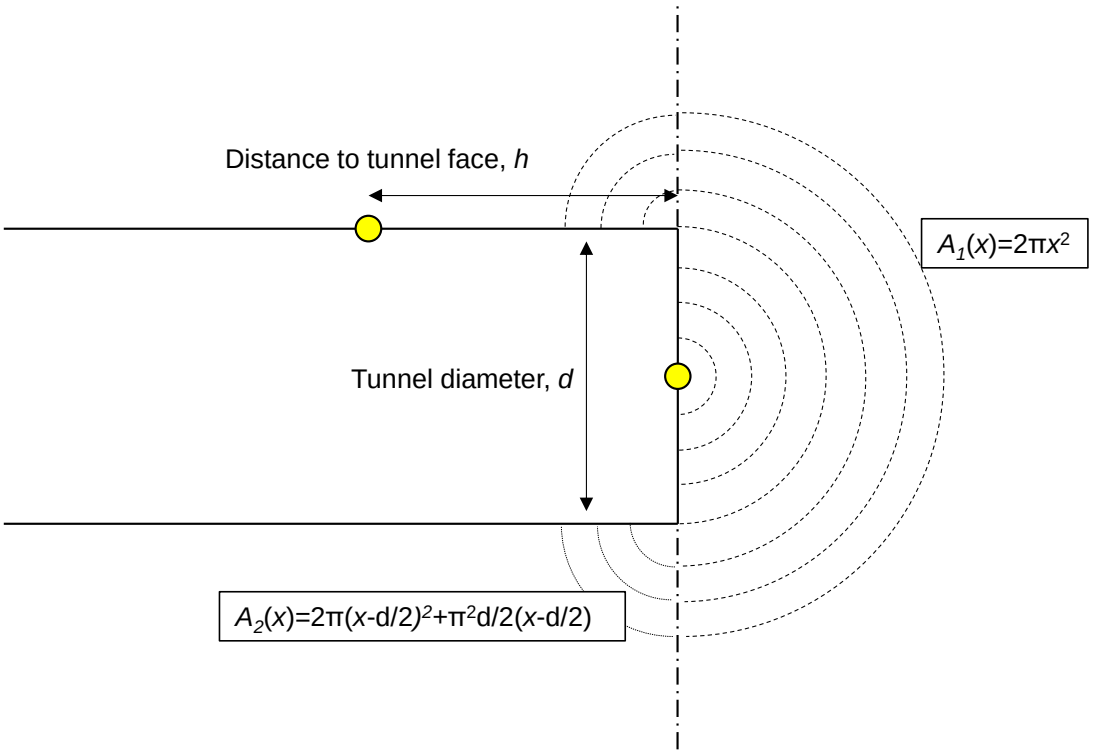

(a) Side view

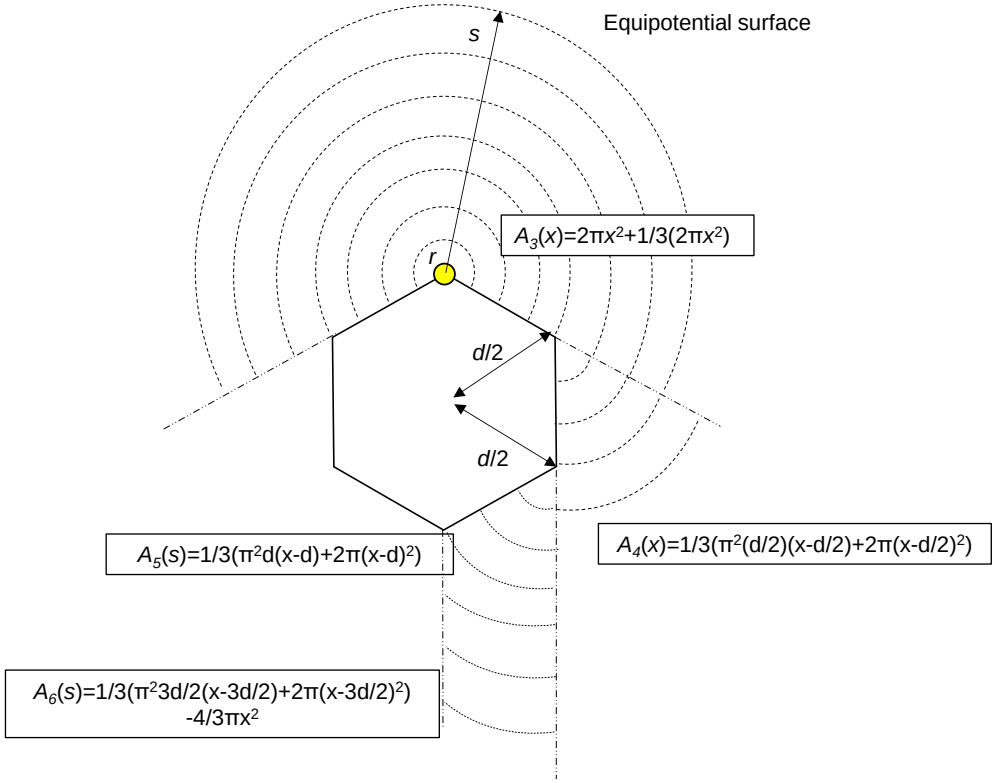

(b) Front view

Fig. 1 Definitions of the symbols

where A, B, C, D, E, F, G, H, J and K which are the geometric constants which are the functions of *d* and *h*. The increment and decrement of the denominator in Eq. (5) is because of the extension and overlap of the equipotential surface (Fig. 2). The sign of the voltages is opposite because two potentials play a role of current inflow and outflow. The electrical resistance between two electrodes on face and wall is obtained by the difference between V_1 and V_2 divided by the electric current (I)

2.2 Electrical Resistance Facing Distinct Medium

There have been many attempts to consider the layered ground during the electrical measurement. In this study, only the conductive (ρ=0) and non-conductive medium (ρ→∞) is assumed ahead of the tunnel face. Valdes (1954) introduced the image method to reflect the effect of the conductive (ρ=0) and non-conductive (ρ→∞) boundary. The basic concept of the image method is the boundary can be replaced by the imaginary electrodes which can make the potential at the boundary zero. This method is employed to simulate the conductive (ρ=0) and non-conductive (ρ→∞) boundary in this study. The sectional shape is also assumed as a hexagonal shape as same as the chapter 2.1. If there is a conductive layer which is vertical to the tun neling direction and is remoted the distance L from the tunnel face which is larger than the half of the diameter (d/2) and smaller than h, the electrical resistance measured from the face and the wall of the tunnel is:

$$V_3=\frac{\rho I}{2\pi}\left(\frac{1}{r}-\frac{1}{d/2}+\underbrace{-\frac{1}{2L}}_{\substack{\text{influence of}\\ \text{image electrode M'}\\ \text{in Fig. 3(a)}}}\right)+\frac{\rho I}{4\pi(B-A)}\left(\begin{array}{l}\ln\left(\dfrac{h+d/2-2r+A}{h+d/2-2r+B}\right)-\ln\left(\dfrac{d/2+A}{d/2+B}\right)\\ \underbrace{+\ln\left(\dfrac{h+\sqrt{(d/2)^2+(2L)^2}-2r+A}{h+\sqrt{(d/2)^2+(2L)^2}-2r+B}\right)-\ln\left(\dfrac{d/2+A}{d/2+B}\right)}_{\text{influence of image electrode N' in Fig. 3(a)}}\end{array}\right) \quad (6)$$

$$\begin{aligned}V_4=&-\frac{\rho I}{\frac{8}{3}\pi}\left(\frac{1}{r}-\frac{1}{d/2}\right)-\frac{\rho I}{\frac{10\pi}{3}(B-A)}\left[\ln\left(\frac{d+C}{d+D}\right)-\ln\left(\frac{d/2+C}{d/2+D}\right)\right]\\&-\frac{\rho I}{4\pi(F-E)}\left[\ln\left(\frac{3d/2+E}{3d/2+F}\right)-\ln\left(\frac{d+E}{d+F}\right)\right]-\frac{\rho I}{\frac{10}{3}\pi(H-G)}\left[\ln\left(\frac{h+G}{h+H}\right)-\ln\left(\frac{3d/2+G}{3d/2+H}\right)\right]\\&-\frac{\rho I}{4\pi(K-J)}\left[\ln\left(\frac{h+d/2-2r+J}{h+d/2-2r+K}\right)\underbrace{-\ln\left(\frac{h+\sqrt{(d/2)^2+(2L)^2}-2r+J}{h+\sqrt{(d/2)^2+(2L)^2}-2r+K}\right)+\ln\left(\frac{2h+2L+J}{2h+2L+K}\right)}_{\text{influence of image electrodes (M' and N' in Fig. 3(a))}}-\ln\left(\frac{h+J}{h+K}\right)\right]\end{aligned} \quad (7)$$

In similar way, the electrical resistance for the ground containing the vertical non-conductive layer can be obtained by changing the sign of the influencing part in Eq. (6) and (7).

3. EXPERIMENTAL TESTS

3.1. Test setup

The scaled model for tunnel excavation is depicted in Fig. 4. This system was

consist of a container, acrylic tunnel, electrodes, LCR meter and steel plate. The medium is brine because it gives a constant electrical resistivity. The electrical resistivity of the brine is 29 Ωm. The size of the container was 0.5 m, 0.5 m, and 0.7 m in width, length, and height. Acrylic hollow tunnel model was cylindrical shape whose outer diameter of 70 mm. An electrode was installed on the center of the face and the other electrode was located on the tunnel wall apart 65 mm, 115 mm, and 165 mm from the tunnel face without protrusion (i.e. circular electrodes). The electrodes with a diameter of 4 mm and a height of 25 mm were made of corrosion-resistant stainless steel and they are not extruded to the brine (i.e. disc). It was connected to LCR meter (Agilent 4263B) that can measure the electrical resistance through the cable and BNC connector. The applied voltage was 1 V and its frequency is 1 kHz to avoid the polarization of the electrodes. The electrical resistance was measured in each 10 mm when tunnel model approached the bottom boundary which simulates the non-conductive boundary and the steel plate which schemed the conductive boundary. The steel plate was 250 mm, 300 mm, and 20 mm in width, length, and height and its resistivity was 7.2×10^{-8} Ωm.

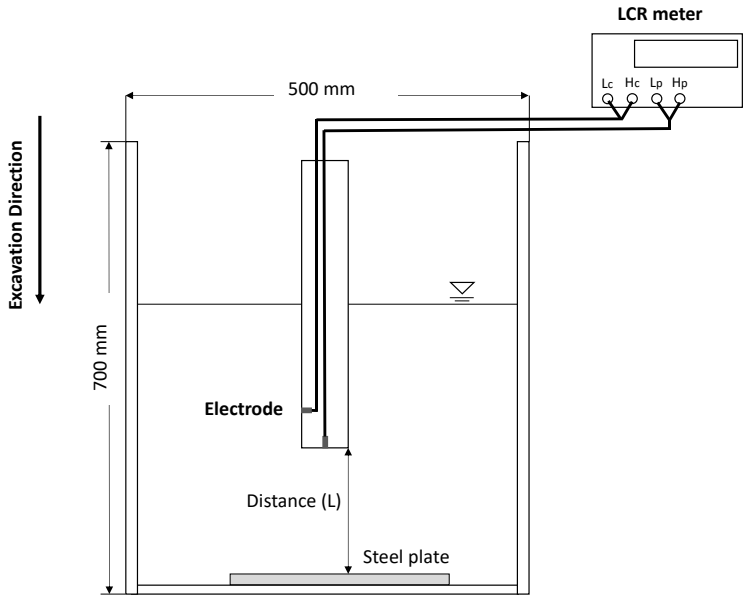

Fig. 2 Test setup

3.2. Results and analysis

The electrical resistance between the electrodes from the tunnel face and wall is slightly influenced by the location of the side wall electrodes because the distance between two electrodes is sufficiently separated. The distance between the tunnel face and the abnormal ground gives a significant effect on the electrical resistance (Fig. 3). Especially in the distance less than 0.05 m, the electrical resistance is affected by the characteristics of the abnormal ground. The electrical resistance decreases when the tunnel approaches the conductive anomaly, however, it increases when the tunnel come close to the non-conductive anomaly. The analytical solution gives the smaller value of the electrical resistance than that from the experimental tests but the trend is

similar. This gap between the electrical resistance from the analytical solution and the experimental test is oriented from the spreading resistance which occurs in the case that the electric current passes the non-uniform cross-section or material. If the difference between the analytical solution and the experimental tests is subtracted, the trend gives an exactly same value each other (Fig. 4(a) and 4(b)).

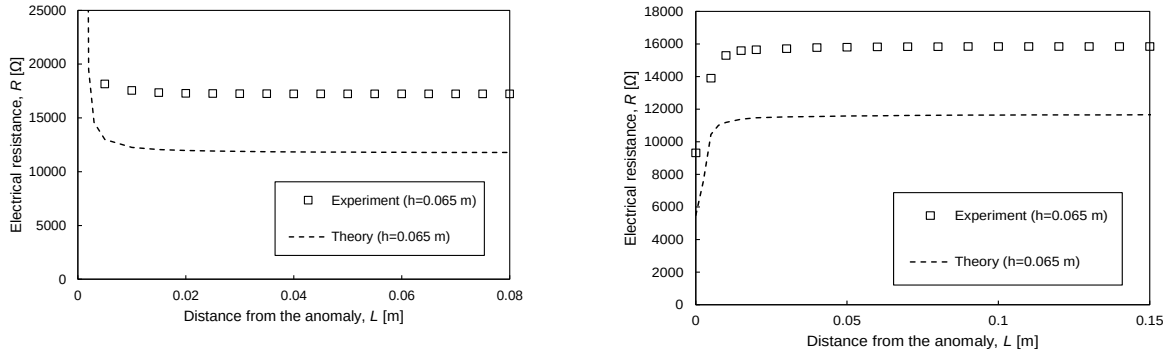

(a) Non-conductive anomaly (b) Conductive anomaly

Fig. 3 Theoretical and experimental resistance

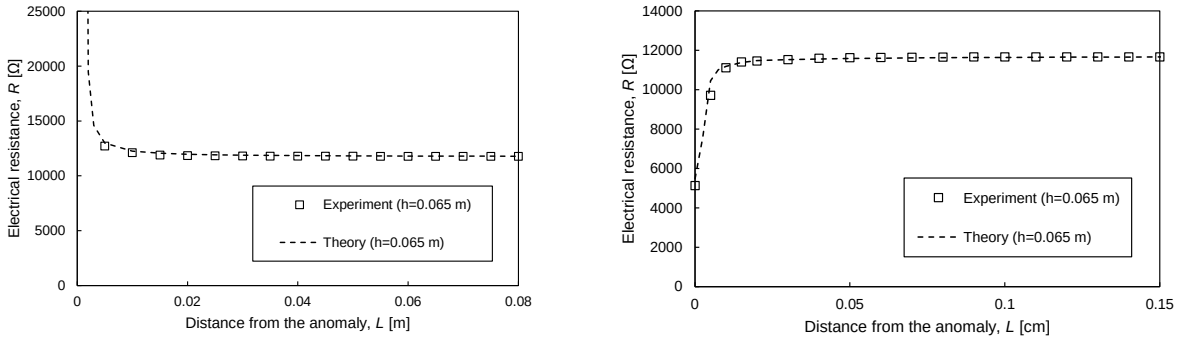

(a) Non-conductive anomaly (b) Conductive anomaly

Fig. 4 Theoretical and experimental resistance

4. CONCLUSIONS

The theoretical resistance between the face and the wall electrodes is derived for the conductive and non-conductive anomaly located ahead of the small diameter TBM. The main conclusions of this study is:

1) The theoretical resistance between two electrodes on the face and the side of the tunnel is derived and compared with the experimental results. The experimental resistance show a similar trends with the theoretical resistance. However, the uniform gap was present between the experimental results and the analytical solution.

2) The gap is oriented by the spreading resistance which is highly dependent on the

size of the electrodes. The spreading resistance is calculated using the theoretical spreading resistance from the references.

ACKNOWLEDGEMENT
This research was supported by Korea Electric Power Corporation (Grant number : R18XA06-09).

REFERENCES

Rowe, P.W. (1972), “The relevance of soil fabric to site investigation practice”, Géotechnique **22**, 195-300.

Li, S., Liu, B., Xu, X., Nie, L., Liu, Z., Song, J., Sun, H., Chen, L., and Fan, K. (2017). “An overview of ahead geological prospecting in tunneling”, Tunnel. and Undergr. Sp. Tech., **63**, 69-94.

Jung, H.S., Choi, J.M., Chun, B.S., Park, J.S., and Lee, Y.J. (2011), “Causes of reduction in shield TBM performance – A case study in Seoul”. Tunnel. and Undergr. Sp. Tech. **26**, 453-461.

Roy, A., and Apparao, A., 1971. Depth of investigation in direct current methods. Geophysics **36**, 943-959.

Schaeffer, K., Mooney, M.A. (2016) “Examining the influence of TBM-ground interaction on electrical resistivity imaging ahead of the TBM”, Tunnel. and Undergr. Sp. Tech., **58**, 82-98.